Inorg. Chem. **2006**, *45*, 5044–5056

Electronic Structure, Spectroscopic Properties, and Reactivity of Molybdenum and Tungsten Nitrido and Imido Complexes with Diphosphine Coligands: Influence of the trans Ligand†

Klaus Mersmann,‡ Andreas Hauser,§ Nicolai Lehnert,‡ and Felix Tuczek*,‡

Institut für Anorganische Chemie, Christian Albrechts Universität, D-24098 Kiel, Germany, and Département de Chimie Physique, Bâtiment de Science II, Université de Genève, 30 quai Ernest Ansermet, 1211 Genève 4, Switzerland

Received January 24, 2006

A series of molybdenum and tungsten nitrido, $[M(N)(X)(diphos)_2]$, and imido complexes, $[M(NH)(X)(diphos)_2)]Y$, (M = Mo, W) with diphosphine coligands (diphos = dppe/depe), various trans ligands ($X = N_3^-$, Cl^-, $NCCH_3$) and different counterions ($Y^- = Cl^-$, BPh_4^-) is investigated. These compounds are studied by infrared and Raman spectroscopies; they are also studied with isotope-substitution and optical-absorption, as well as emission, spectroscopies. In the nitrido complexes with *trans*-azido and -chloro coligands, the metal–N stretch is found at about 980 cm^{-1}; upon protonation, it is lowered to about 920 cm^{-1}. The $^1A_1 \rightarrow {}^1E$ ($n \rightarrow \pi^*$) electronic transition is observed for $[Mo(N)(N_3)(depe)_2]$ at 398 nm and shows a progression in the metal–N stretch of 810 cm^{-1}. The corresponding $^3E \rightarrow {}^1A$ ($\pi^* \rightarrow n$) emission band is observed at 542 nm, exhibiting a progression in the metal–N stretch of 980 cm^{-1}. In the imido system $[Mo(NH)(N_3)(depe)_2]BPh_4$, the $n \rightarrow \pi^*$ transition is shifted to lower energy (518 nm) and markedly decreases in intensity. In the *trans*-nitrile complex $[Mo(N)(NCCH_3)(dppe)_2]BPh_4$, the metal–N(nitrido) stretching frequency increases to 1016 cm^{-1}. The $n \rightarrow \pi^*$ transition now is found at 450 nm, shifting to 525 nm upon protonation. Most importantly, the reduction of this nitrido *trans*-nitrile complex is drastically facilitated compared to its counterparts with anionic *trans*-ligands ($E_p^{red} = -1.5$ V vs Fc^+/Fc). On the other hand, the basicity of the nitrido group is decreased ($pK_a\{[Mo(NH)(NCCH_3)(dppe)_2](BPh_4)_2\} = 5$). The implications of these findings with respect to the Chatt cycle are discussed.

1. Introduction

The transition-metal-mediated conversion of dinitrogen to ammonia under ambient conditions is a subject of continuing interest.[1] Recently, Yandulov and Schrock succeeded in catalytically performimg this reaction using a Mo(III) complex with a sterically shielding triamidoamine ligand.[2] With decamethylchromocene as the reductant and lutidinium BAr'_4 as the acid ($Ar' = 3,5\text{-}(CF_3)_2C_6H_3$), they were able to generate NH_3 from N_2 at room temperature and normal pressure, achieving 6 cycles with an overall yield of 65%. On the basis of the available experimental information, a mechanism was proposed for this reaction (*Schrock cycle*)[2] and reproduced by DFT calculations.[3]

Many years before, Pickett and Talarmin, in a classic experiment, had already succeeded in producing ammonia from N_2 in a cyclic fashion; however, it was a stepwise procedure with a much lower yield.[4] Their process was based on the complex $[W(NNH_2)TsO(dppe)_2]^+$ ($TsO = p\text{-}CH_3C_6H_4SO_3^-$) which was electrolyzed to give the parent dinitrogen complex $[W(N_2)_2(dppe)_2]$, ammonia, and H_2. Protonation of the bis(dinitrogen) complex reformed the starting complex; this procedure was repeated twice. The

† Reduction and protonation of end-on terminally coordinated dinitrogen. Part VI.

* To whom correspondence should be addressed. E-mail: ftuczek@ac.uni-kiel.de.

‡ Christian Albrechts Universität.

§ Université de Genève.

(1) MacKay, B. A.; Fryzuk, M. D. *Chem. Rev.* **2004**, *104*, 385.

(2) (a) Yandulov, D. V.; Schrock, R. R. *J. Am. Chem. Soc.* **2002**, *124*, 6252. (b) Yandulov, D. V.; Schrock, R. R.; Rheingold, A. L.; Ceccarelli, C.; Davis, W. M. *Inorg. Chem.* **2003**, *42*, 796. (c) Yandulov, D. V.; Schrock, R. R. *Science* **2003**, *301*, 76. (d) Ritleng, V.; Yandulov, D. V.; Weare, W. W.; Schrock, R. R.; Hock, A. S.; Davis, W. M. *J. Am. Chem. Soc.* **2004**, *126*, 6150. (e) Yandulov, D. V.; Schrock, R. R. *Inorg. Chem.* **2005**, *44*, 1103. (f) Yandulov, D. V.; Schrock, R. R. *Inorg. Chem.* **2005**, *44*, 5542. (g) Yandulov, D. V.; Schrock, R. R. *Can. J. Chem.* **2005**, *83*, 341.

(3) Studt, F.; Tuczek, F. *Angew. Chem., Int. Ed.* **2005**, *44*, 5639.

(4) (a) Pickett, C. J.; Talarmin, J. *Nature* **1985**, *317*, 652. (b) Pickett, C. J.; Ryder, K. S.; Talarmin, J. *J. Chem. Soc., Dalton Trans.* **1986**, *7*, 1453.

10.1021/ic060141n CCC: $33.50
Published on Web 05/25/2006

Scheme 1

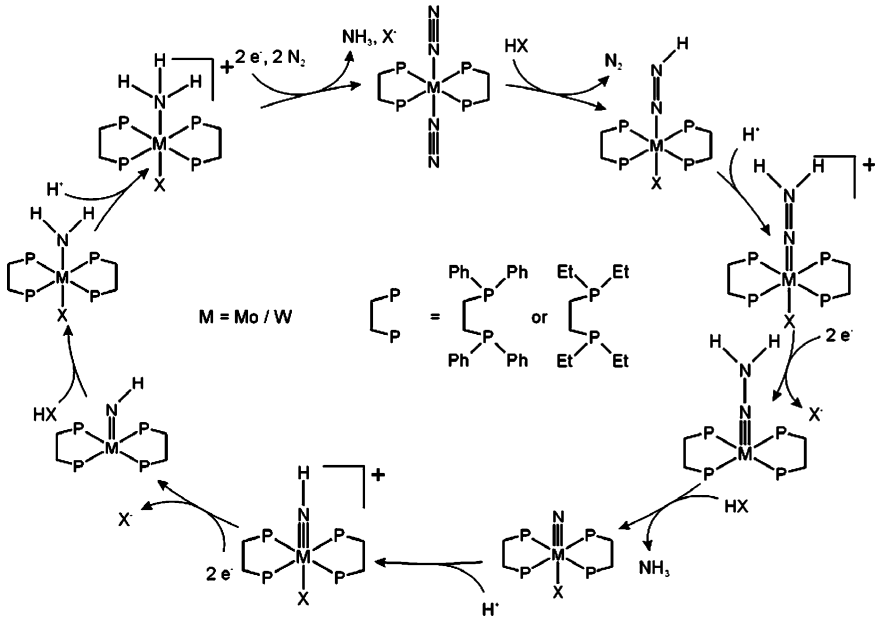

corresponding chemistry proceeds within the *Chatt cycle*, which provided the first complete scheme for the transition-metal-mediated conversion of N_2 to ammonia (Scheme 1).[5] The first two steps of this cycle involve the protonation of molybdenum and tungsten dinitrogen complexes with diphosphine coligands to give the corresponding NNH_2 complexes. We have investigated the molybdenum and tungsten N_2, NNH, and NNH_2 intermediates appearing in this chemistry by a variety of spectroscopic methods coupled to DFT calculations.[6] In the presence of strong acids, an additional proton can be added giving NNH_3 (hydrazidium) species.[7] At this stage, the N−N triple bond of N_2 has been reduced to a single bond and can be cleaved by adding two electrons from an external reductant or electrochemically. Alternatively, two-electron reduction can be performed at the NNH_2 stage, leading to the elimination of the trans ligand and formation of five-coordinate Mo(II) intermediates. This process has been studied on the basis of alkylated derivatives.[8] If the doubly reduced, five-coordinate intermediates, $[M(II)(dppe)_2NNR_2]$, are protonated, the N−N bond cleaves, and secondary amines, as well as M(IV) nitrido or imido complexes, are formed.[9] We spectroscopically and kinetically followed the splitting of the N−N bond and explored various mechanistic scenarios to account for the experimental observations.[10]

In the second part of the Chatt cycle, Mo and W nitrido complexes have to be converted to the corresponding low-valent ammine complexes that are able to exchange NH_3 against N_2. One of the problems associated with this chemistry are the strongly negative potentials which, in particular, are needed to regenerate the +I and zerovalent Mo and W species.[11] The presence of such negative potentials accounts for the large fraction of H_2 that is formed from the acids employed in these experiments (vide supra). One of the possibilities to shift the reduction potentials to less negative values is to use a weakly donating or even labile ligand in the trans position to the nitrido/imido group. Replacing, for example, halide by acetonitrile (i) increases the total charge of the complex because of the exchange of a negatively charged by a neutral ligand, (ii) increases the effective nuclear charge, Z_{eff}, of the metal center because of a decreased ligand σ/π donor strength, and in particular (iii), lowers the d_{xz}/d_{yz} orbitals of the metal centers because of the lack of π-donor capability. All of these effects should act to make the nitrido complex easier to reduce (i.e., shift the reduction potential to less negative values).

Herein, we investigate the influence of the trans ligand on the electronic structure, the spectroscopic properties and reactivity of the molybdenum and tungsten nitrido complexes. To this end, a series of molybdenum and tungsten nitrido and imido complexes with dppe and depe coligands and trans ligands of different σ/π-donor strengths (azide, chloride, acetonitrile) is investigated by UV−vis, IR, and Raman spectroscopies and electrochemistry. The results are interpreted by means of DFT calculations, and the general implications with respect to a catalytic ammonia synthesis on the basis of the Chatt cycle are discussed.

2. Experimental Section

Sample Preparation and Isotopic Substitution. A set of molybdenum and tungsten nitrido complexes with dppe as the coligand was synthesized (i.e., the trans azido complexes [Mo(N)-

(5) (a) Henderson, R. A.; Leigh, G. J.; Pickett, C. J. *Adv. Inorg. Chem. Radiochem.* **1983**, *27*, 197. (b) Pickett, C. J. *J. Biol. Inorg. Chem.* **1996**, *1*, 601.
(6) (a) Lehnert, N.; Tuczek, F. *Inorg. Chem.* **1999**, *38*, 1659. (b) Lehnert, N.; Tuczek, F. *Inorg. Chem.* **1999**, *38*, 1671.
(7) (a) Galindo, A.; Hills, A.; Hughes, D. L.; Richards, R. L. *J. Chem. Soc., Chem. Commun.* **1987**, 1815. (b) Horn, K. H.; Lehnert, N.; Tuczek, F. *Inorg. Chem.* **2003**, *42*, 1076.
(8) Hussain, W.; Leigh, G. J.; Pickett, C. J. *J. Chem. Soc., Chem. Commun.* **1982**, 747.
(9) Henderson, R. A.; Leigh, G. J.; Pickett, C. J. *J. Chem. Soc., Dalton Trans.* **1989**, 425.
(10) Mersmann, K.; Horn, K. H.; Böres, N.; Lehnert, N.; Studt, F.; Paulat, F.; Peters, G.; Tuczek, F. *Inorg. Chem.* **2005**, *44*, 3031.
(11) Alias, Y.; Ibrahim, S. K.; Queiros, M. A.; Fonseca, A.; Talarmin, J.; Volant, F.; Pickett, C. J. *J. Chem. Soc., Dalton Trans.* **1997**, 4807.

$(N_3)(dppe)_2]$ (**1**) and $[W(N)(N_3)(dppe)_2]$ (**2**), as well as the trans chloro complexes $[Mo(N)(Cl)(dppe)_2]$ (**3**) and $[W(N)(Cl)(dppe)_2]$ (**4**)). These complexes were prepared by following literature procedures.[12] Another reaction route,[8,9,13] starting from $[W(^{15}N_2)_2(dppe)_2]$, was employed to prepare the ^{15}N isotopomer of complex **4** (**4**(^{15}**N**)). Furthermore we synthesized the depe complex $[Mo(N)(N_3)(depe)_2]$ (**5**)[14] and the trans acetonitrile complex $[Mo(N)(NCCH_3)(dppe)_2]BPh_4$ (**6**).[9]

Protonation of the nitrido complexes, **No** (No = 1, 2, ..., 6), was performed with various acids HX, leading to the imido derivatives **No*HX**. Condensation of dry HCl gas on frozen dichloromethane solutions of the **No** complexes gave the chloro−imido complexes **No*HCl** (No = 2, 3, 4). The products were precipitated by adding hexane to the solutions. DCl gas was used to generate the deuterated counterparts, **No*DCl** (No = 2, 3, 4). Imido complexes with tetraphenylborate as counterion (**No*HBPh$_4$**) were prepared using lutidinium tetraphenylborate ($HLutBPh_4$) as acid in thf (No = 1, 2, 5, 6). The products were obtained upon addition of methanol and diethyl ether to the solutions. Treatment with methanol-d_1 was used to convert the imido complexes to their deuterated counterparts, **No*DBPh$_4$** (No = 1, 2, 5).

All reactions and sample preparations were performed under a nitrogen or argon atmosphere using Schlenk techniques. All solvents were dried under argon. Sample manipulations for vibrational and optical spectroscopy were carried out in a glovebox.

Elemental Analyses. The elemental analyses were performed on a CHN-O-RAPID (Heraeus) instrument in little tin containers (Elementar). Observed C/H/N values (calcd values):[15] **1** 65.7/6.4/5.1 (65.8/5.1/5.9), **2** 59.5/5.2/5.9 (60.2/4.7/5.4), **4** 59.3/4.9/1.4 (60.6/4.7/1.4), **4**(^{15}**N**) 58.9/4.7/1.5 (60.6/4.7/1.4), **5** 41.3/8.3/8.5 (42.6/8.6/9.9), **6** 74.4/7.2/2.3 (73.9/5.7/2.2), **2*HCl** 56.5/5.2/4.4 (58.2/4.6/5.2), **3*HCl** 63.1/6.0/1.5 (63.8/5.1/1.4), **4*HCl** 56.6/5.1/1.4 (58.6/4.6/1.3), **1*HBPh$_4$** 70.9/6.2/3.9 (71.9/5.5/4.4), **2*HBPh$_4$** 67.9/6.0/3.5 (67.3/5.1/4.1), **5* HBPh$_4$** 59.8/8.6/6.0 (59.7/7.9/6.3).

Spectroscopic Instrumentation. FT-IR spectra were recorded in KBr pellets on a Mattson Genesis type I spectrometer. Optical absorption spectra of solutions were recorded on a Analytic Jena Specord S100 spectrometer. UV−vis spectra on neat compounds pressed between sapphire windows were recorded at 10 K using a Varian Cary 5 UV−vis−NIR spectrometer equipped with a CTI cryocooler. Luminescence spectra were measured with a SPEX Fluorolog System equipped with an optical helium cryostat (λ_{ex} = 400 nm).

Luminescence Spectra of [Mo(N)(N$_3$)(depe)$_2$] (5). A little drop of rubber cement was put on a small copper plate to hold a dense layer of polycrystalline material. At 11 K, strong luminescence was observed. A cross-check with a drop of rubber cement without compound **5** gave a vanishing intensity at 11 K, proving that the luminescence in fact derives from $[Mo(N)(N_3)(depe)_2]$. The luminescence intensity is strongly temperature dependent and at 77 K already quite weak.

Electrochemical Investigations. Cyclic voltammograms were recorded with an EG and G PAR model 273A potentiostat controlled by EG and G PAR M270 software using a Pt knob working electrode, a Pt counter electrode, and a silver reference electrode. A solution of $[MoN(NCCH_3)(dppe)_2]BPh_4$ (0.5 mM) and $[NBu_4][PF_6]$ (0.1M) in acetonitrile was recorded at 25 °C. The scan rate was set to 100 mVs^{-1}. The potentials are referenced against ferrocenium−ferrocene.

Normal Coordinate Analysis. Normal coordinate calculations were performed using the QCPE computer program by Peterson and McIntosh. It involves solutions of the secular equation $GFL = \Lambda L$ by the diagonalization procedure of Miyazawa.[16] The calculations are based on a general valence force field, and the force constants are refined using the nonlinear optimization of the simplex algorithm according to Nelder and Mead.[17] Normal coordinate analysis is based on the QCB−NCA procedure which involves generation of an initial force field by DFT methods.[6]

DFT Calculations. Spin-restricted DFT calculations were performed for the nitrido systems, $[Mo(N)(N_3)(diphos)_2]$ (**I**), $[Mo(N)(Cl)(diphos)_2]$ (**III**), and $[Mo(N)(NCCH_3)(diphos)_2]^+$ (**VI**), and for the corresponding imido systems, $[Mo(NH)(N_3)(diphos)_2]^+$ (**I*H**$^+$), $[Mo(NH)(Cl)(diphos)_2]^+$ (**III*H**$^+$), and $[Mo(NH)(NCCH_3)(diphos)_2]^{2+}$ (**VI*H**$^+$), using Becke's three parameter hybrid functional with the correlation functional of Lee, Yang, and Parr (B3LYP).[18] All diphosphine ligands (dppe, depe) are simplified to $H_2PCH_2CH_2PH_2$ ("diphos"). **I**, **III**, and **VI** are models of compounds **1**/**2**/**5**, **3**/**4**, and **6**, respectively, whereas **I*H**$^+$, **III*H**$^+$, and **VI*H**$^+$ are models of compounds **1*HBPh$_4$**/**2*HBPh$_4$**/**5*HBPh$_4$**, **3*HBPh$_4$**/**4*HBPh$_4$**, and **6*HBPh$_4$**, respectively. The LANL2DZ basis set was used for the calculations. It applies the Dunning/Huzinaga full double-ζ[19] basis functions on the first row and the Los Alamos effective core potentials plus DZ functions on all other atoms.[20] Charges were analyzed using the natural bond orbital (NBO) formalism (natural population analysis, NPA).[21] All computational procedures were used as implemented in the Gaussian 98 package.[22] Wave functions were plotted with GaussView. The ***f*** matrix in internal coordinates was extracted from the Gaussian output using the program REDONG.[23]

(12) (a) Dilworth, J. R.; Richards, R. L. *Inorg. Synth.* **1980**, *20*, 119. (b) George, T. A.; Noble, M. E. *Inorg. Chem.* **1978**, *17*, 1678. (c) Chatt, J.; Dilworth, J. R. *J. Chem. Soc., Chem. Commun.* **1975**, 983. (d) Chatt, J.; Dilworth, J. R. *J. Indian Chem. Soc.* **1977**, *54*, 13. (e) Bevan, P. C.; Chatt, J.; Dilworth, J. R.; Henderson, R. A.; Leigh, G. J. *J. Chem. Soc., Dalton Trans.* **1982**, 821.

(13) Chatt, J.; Hussain, W.; Leigh, G. J.; Terreros, F. P. *J. Chem. Soc., Dalton Trans.* **1980**, 1408.

(14) (a) Hussain, W.; Leigh, G. J.; Ali, H. M.; Pickett, C. J.; Rankin, D. A. *J. Chem. Soc., Dalton Trans.* **1984**, 1703. (b) Hughes, D. L.; Mohammed, M. Y.; Pickett, C. J. *J. Chem. Soc., Dalton Trans.* **1990**, 2013.

(15) Larger deviations between the calculated and observed values are observed for compounds **1** and **6**. As evident from NMR, the deviations in compound **1** are the result of trimethylsilyl impurities. Trimethylsilyl azide was added to convert $[Mo(N_2)_2(dppe)_2]$ to $[MoN(N_3)(dppe)_2]$ (**1**). In compound **6**, the deviation is caused by an admixture of $HNEt_3BPh_4$; triethylamine was added as a base to deprotonate $[Mo(NH)Cl(dppe)_2]Cl$ and $NaBPh_4$ was added to precipitate $[Mo(N)(CH_3CN)(dppe)_2]BPh_4$ (**6**).

(16) Miyazawa, T. J. *Chem. Phys.* **1958**, *29*, 246.

(17) Nelder, J. A.; Mead, R. *Comput. J.* **1965**, *7*, 308.

(18) Becke, A. D. *J. Chem. Phys.* **1993**, *98*, 5648.

(19) Dunning, T. H., Jr.; Hay, P. J. In *Modern Theoretical Chemistry*; Schaefer, H. F., III, Ed.; Plenum: New York, 1976.

(20) (a) Hay, P. J.; Wadt, W. R. *J. Chem. Phys.* **1985**, 82, 270, 299. (b) Wadt, W. R.; Hay, P. J. *J. Chem. Phys.* **1985**, *82*, 284.

(21) (a) Foster, J. P.; Weinhold, F. *J. Am. Chem. Soc.* **1980**, *102*, 7211. (b) Rives, A. B.; Weinhold F. *Int. J. Quantum Chem. Symp.* **1980**, *14*, 201. (c) Reed, A. E.; Weinstock, R. B.; Weinhold, F. *J. Chem. Phys.* **1985**, *83*, 735. (d) Reed, A. E.; Curtiss, L. A.; Weinhold, F. *Chem. Rev.* **1988**, *88*, 899.

(22) Frisch, M. J.; Trucks, G. W.; Schlegel, H. B.; Scuseria, G. E.; Robb, M. A.; Cheeseman, J. R.; Zakrzewski, V. G.; Montgomery, J. A., Jr.; Stratmann, R. E.; Burant, J. C.; Dapprich, S.; Millam, J. M.; Daniels, A. D.; Kudin, K. N.; Strain, M. C.; Farkas, O.; Tomasi, J.; Barone, V.; Cossi, M.; Cammi, R.; Mennucci, B.; Pomelli, C.; Adamo, C.; Clifford, S.; Ochterski, J.; Petersson, G. A.; Ayala, P. Y.; Cui, Q.; Morokuma, K.; Malick, D. K.; Rabuck, A. D.; Raghavachari, K.; Foresman, J. B.; Cioslowski, J.; Ortiz, J. V.; Stefanov, B. B.; Liu, G.; Liashenko, A.; Piskorz, P.; Komaromi, I.; Gomperts, R.; Martin, R. L.; Fox, D. J.; Keith, T.; Al-Laham, M. A.; Peng, C. Y.; Nanayakkara, A.; Gonzalez, C.; Challacombe, M.; Gill, P. M. W.; Johnson, B. G.; Chen, W.; Wong, M. W.; Andres, J. L.; Head-Gordon, M.; Replogle, E. S.; Pople, J. A. *Gaussian 98;* Gaussian, Inc.: Pittsburgh, PA, 1998.

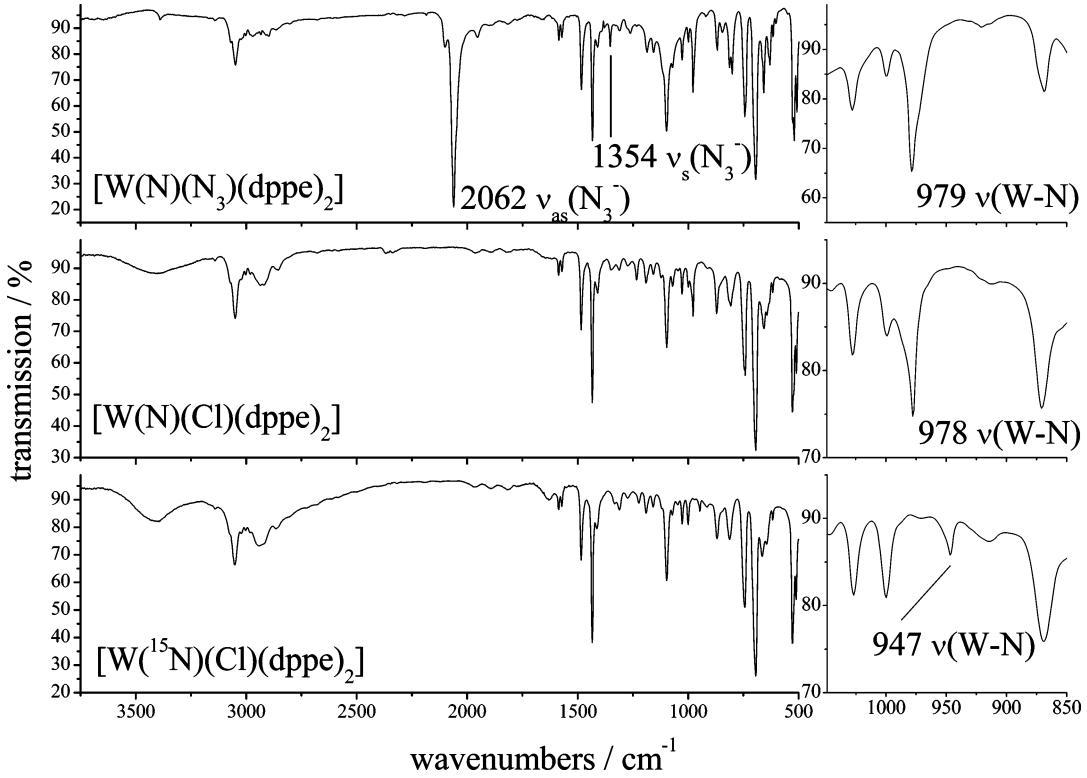

Figure 1. IR spectra of nitrido complexes $[W(N)(N_3)(dppe)_2]$ (**2**), $[W(N)(Cl)(dppe)_2]$ (**4**), and $[W(^{15}N)(Cl)(dppe)_2]$ (**4(15N)**).

3. Results and Analysis

Vibrational Spectroscopy and DFT Frequency Analysis. The infrared spectra of the tungsten−dppe nitrido complexes, $[W(N)(N_3)(dppe)_2]$ (**2**) and $[W(N)(Cl)(dppe)_2]$ (**4**), are presented in Figure 1, along with the IR spectrum of the ^{15}N isotopomer of **4**, **4(15N)**. On the right-hand side of Figure 1, the region between 850 cm^{-1} and 1050 cm^{-1} is presented on a larger scale. The spectrum of the *trans*-azido−nitrido complex **2** is dominated by the antisymmetric N−N vibration of the azide ligand, $\nu_{as}(N_3^-)$, at 2062 cm^{-1}. Its symmetric counterpart, $\nu_s(N_3^-)$, can be found at 1354 cm^{-1}. The metal−nitrido stretching vibration is located at 979 cm^{-1}. The remaining bands are mostly caused by vibrations of the dppe ligand. The IR spectrum of the molybdenum analogue of **2**, $[Mo(N)(N_3)(dppe)_2]$ (**1**, not shown), is very similar (i.e., the antisymmetric azide vibration is found at 2051 cm^{-1}, the corresponding symmetric mode is at 1348 cm^{-1}, and the metal−nitrido stretching vibration appears at 975 cm^{-1}). As is evident from the spectrum of the nitrido−chloro complex $[W(N)(Cl)(dppe)_2]$ (**4**), exchange of the trans ligand from azide to chloride has almost no effect on the position of the metal−nitrido vibration, which appears in the spectrum of **4** at 978 cm^{-1}. In the ^{15}N isotopomer $[W(^{15}N)(Cl)(dppe)_2]$, **4(15N)**, this vibration shifts by about 30 cm^{-1} to 947 cm^{-1}.

In Figure 2, the infrared spectra of $[Mo(NH)(N_3)(depe)_2]$-BPh_4 (**5*HBPh4**) and $[Mo(ND)(N_3)(depe)_2]BPh_4$ (**5*DBPh4**) are presented along with the spectrum of the parent nitrido complex $[Mo(N)(N_3)(depe)]$ (**5**). In the latter system, the metal−N vibration is easily identified at 980 cm^{-1}; the symmetric azide stretch is located at 1328 cm^{-1}, whereas the antisymmetric combination is found at 2029 cm^{-1}. In the spectrum of the imido complex, these peaks are shifted to 1376 and 2080 cm^{-1}, respectively. The metal−N stretch shifts to 922 cm^{-1}. Upon deuteration, this signal shifts to 892 cm^{-1}. The decrease of the metal−(NH) stretching frequency upon deuteration is due to an increasing mass of the NH moiety by one, and therefore, it has an effect comparable to the ^{15}N substitution in the nitrido complex. At 3250 cm^{-1}, a broad band can be identified, which in the deuterated complex is shifted to 2430 cm^{-1}. This signal derives from the imido N−H stretching vibration and an O−H stretch which is associated with methanol being present as a crystal solvent. Unfortunately, attempts to isolate the imido complex in the absence of methanol failed. In addition to the nitrido complex, the spectra of the imido system also contain the signals of the counterion, tetraphenylborate. The Raman spectra of these compounds, which are given in Figure S1 (Supporting Information), exhibit bands at similar positions. The results of the IR and Raman experiments are collected in Table 1.

A DFT frequency analysis of the optimized model $[Mo(N)(N_3)(diphos)_2]$ (**I**) of **1**/**2**/**5** predicts a frequency of 1049 cm^{-1} for the metal−N stretch, slightly higher than the observed value. This corresponds to the finding that the metal−N distance is calculated slightly too short (see below). The frequency analysis further provides an ***f*** matrix which is used as an initial guess for a normal coordinate analysis (quantum chemistry-based normal coordinate analysis, QCB-NCA).[6] The results of the fitting procedure are collected in Table 2. In particular, the fitting of the metal−N stretch to the experimental value gives a corresponding force constant of 7.065 mdyn/Å.

(23) Allouche, A.; Pourcin, J. *Spectrochim. Acta* **1993**, *49A*, 571.

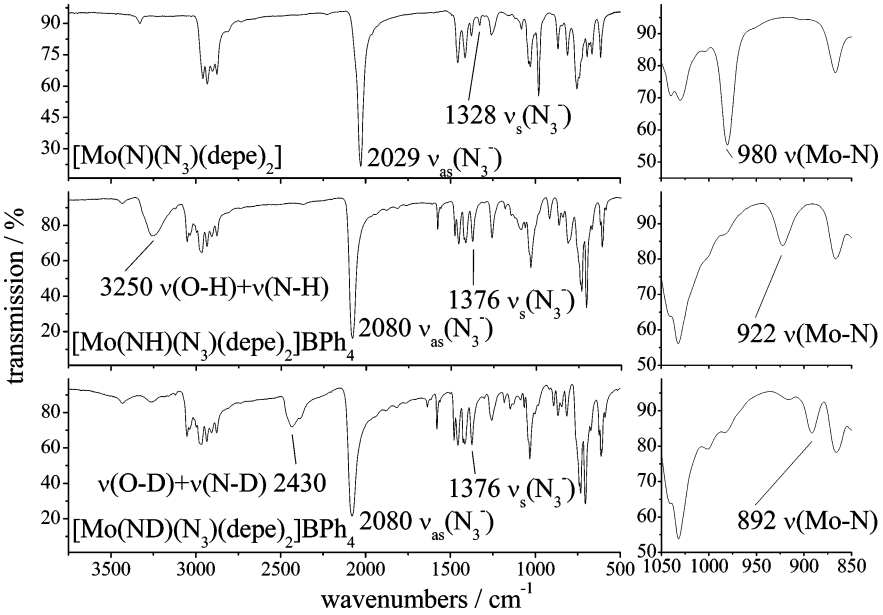

Figure 2. IR spectra of nitrido and imido complexes with molybdenum and depe and a tetraphenylboron counterion: $[Mo(N)(N_3)(depe)_2]$ (**5**), $[Mo(NH)(N_3)(depe)_2]BPh_4$ (**5*HBPh$_4$**), and $[Mo(ND)(N_3)(depe)_2]BPh_4$ (**5*DBPh$_4$**).

Table 1. Comparison of Metal−N, N−H, Symmetric (sym) N_3^-, and Antisymmetric (asym) N_3^- Vibrations in Different Nitrido and Imido Complexes[a]

		M−N	N−H	sym N_3^-	asym N_3^-
$[Mo(N)(N_3)(dppe)_2]$	**1**	975		1348	2051
$[W(N)(N_3)(dppe)_2]$	**2**	979		1354	2062
$[W(N)(Cl)(dppe)_2]$	**4**	978			
$[W(^{15}N)(Cl)(dppe)_2]$	**4(^{15}N)**	947			
$[Mo(N)(N_3)(depe)_2]$	**5**	980		1330	2029
$[Mo(N)(NCCH_3)(dppe)_2]BPh_4$	**6**	1016			
$[W(NH)(N_3)(dppe)_2]Cl$	**2*HCl**	950	2500−3000	1390	2093
$[W(ND)(N_3)(dppe)_2]Cl$	**2*DCl**	912	1750−2250	1391	2093
$[Mo(NH)(Cl)(dppe)_2]Cl$	**3*HCl**	950	2500−3000		
$[Mo(ND)(Cl)(dppe)_2]Cl$	**3*DCl**	910	1750−2250		
$[W(NH)(Cl)(dppe)_2]Cl$	**4*HCl**	946	2350−3100		
$[W(ND)(Cl)(dppe)_2]Cl$	**4*DCl**	916	1800−2250		
$[Mo(NH)(N_3)(dppe)_2]BPh_4$	**1*HBPh$_4$**	905	3250	1387	2092
$[W(NH)(N_3)(dppe)_2]BPh_4$	**2*HBPh$_4$**	920	3300	1395	2104
$[W(ND)(N_3)(dppe)_2]BPh_4$	**2*DBPh$_4$**	891	2470	1395	2104
$[Mo(NH)(N_3)(depe)_2]BPh_4$	**5*HBPh$_4$**	924	3250	1376	2080
$[Mo(ND)(N_3)(depe)_2]BPh_4$	**5*DBPh$_4$**	893	2430	1376	2080
$[Mo(NH)(NCCH_3)_2](BPh_4)_2$	**6*HBPh$_4$**	925	3150−3350		

[a] All data given in cm^{-1}.

Table 2. Vibrational Data of Nitrido and Imido Complexes and Comparison to Calculated Results and Force Constants

$[Mo(N)(N_3)(diphos)_2]$	exptl (cm^{-1})	B3LYP (cm^{-1})	NCA (cm^{-1})	*f*(NCA) (mdyn/Å)
Mo−N	980	1049	980 cm^{-1}	7.065
Mo−^{15}N	947	1019	951	
Mo−N (^{1}E exc. st.)	810		810	4.9
$[Mo(NH)(N_3)(diphos)_2]^+$	exptl (cm^{-1})	B3LYP (cm^{-1})	NCA (cm^{-1})	*f* (NCA) (mdyn/Å)
N−H	3250	3586	3261	5.848
N−D	2430	2639	2402	
Mo−NH	924	964	924	6.700
Mo−ND	893	932	892	

A DFT frequency analysis was also performed for the imido−azido model system $[Mo(NH)(N_3)(diphos)_2]^+$ (**I*H$^+$**) of compounds **1*HBPh$_4$**, **2*HBPh$_4$**, and **5*HBPh$_4$**. The calculated metal−N vibrational frequencies of 964 cm^{-1} for the protonated and 932 cm^{-1} for the deuterated complexes are again somewhat too high, as found for the nitrido complexes. The N−H stretching vibration is calculated to be 3586 cm^{-1}, and the N−D stretch is calculated to be 2639 cm^{-1}, also higher than observed. After normal coordinate analysis, force constants of 6.7 mdyn/Å for the metal−N and 5.848 mdyn/Å for the N−H bonds are obtained. This demonstrates that the strength of the metal−N bond is only slightly (i.e., by 0.365 mdyn/Å) reduced upon protonation. Table 2 shows the results of this analysis.

Counterions which form hydrogen bridges with the imido proton have an influence on the metal−(NH) and N−H vibrations. This can be seen in the spectral pattern of the N−H vibration in $[W(NH)(Cl)(dppe)_2]Cl$ (**4*HCl**) (Figure S2, Supporting Information), which appears in the range between 2400 and 2900 cm^{-1}. In this case, the metal−(NH) vibration is centered at 946 cm^{-1} and appears to be split. In the deuterated complex, the signal intensities are markedly decreased. The N−D vibration appears in the range between 1750 and 2200 cm^{-1}, and the metal−N vibration is shifted

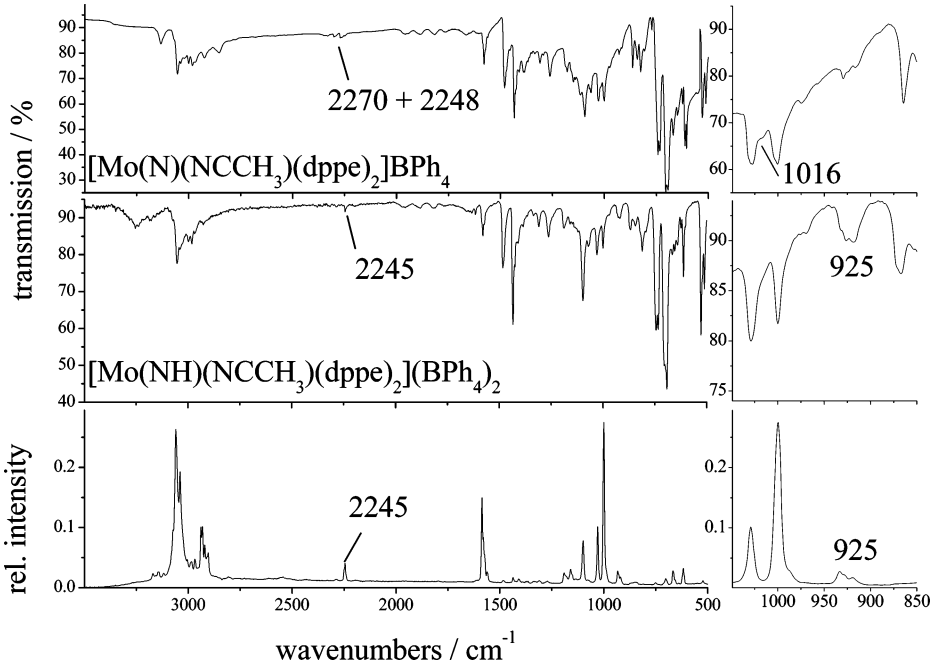

Figure 3. IR spectrum of nitrido-*trans*-nitrile complex $[Mo(N)(NCCH_3)(dppe)_2]BPh_4$ (**6**) with IR and Raman spectra of the protonated product, $[Mo(NH)(NCCH_3)(dppe)_2](BPh_4)_2$ (**6*HBPh$_4$**).

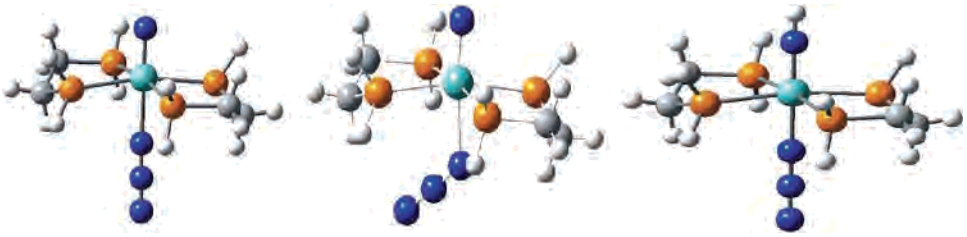

Figure 4. Geometry-optimized structures of $[Mo(N)(N_3)(PH_2CH_2CH_2PH_2)_2]$ (**I**) (left), **I (^{3}E exc. st.)** (middle), and $[Mo(NH)(N_3)(PH_2CH_2CH_2PH_2)_2]^+$ (**I*H**$^+$) (right).

to 916 cm^{-1}. The positions of the metal−N vibrations for the systems with chloride as counterion are reproduced by the Raman spectra of **2*HCl** and **2*DCl** (Figure S3) which exhibit these vibrations at 950 cm^{-1} for the protonated and 912 cm^{-1} for the deuterated complexes.

Finally, the IR and Raman spectra of complexes with trans nitrile ligands were recorded (Figure 3). In these systems, the IR spectrum of the nitrido complex $[Mo(N)(NCCH_3)(dppe)_2]BPh_4$ (**6**) exhibits weak bands at 2270 and 2248 cm^{-1} which are attributed to coordinated acetonitrile. At 1016 cm^{-1}, a shoulder appears which could be associated with the metal−N stretch. A more definitive assignment is difficult because of the intense bands at 1000 and 1030 cm^{-1}, which originate from the aromatic ligands. Unfortunately, no complementary information with respect to this problem could be derived from the corresponding Raman spectrum. Because of the low basicity of this complex (see below), the protonated species, $[Mo(NH)(NCCH_3)(dppe)_2](BPh_4)_2$ (**6*HBPh$_4$**), is only obtained as a mixture with the protonating agent lutidinium tetraphenylborate. The corresponding sample does not exhibit the shoulder at 1016 cm^{-1}. Instead, new bands at 932 and 920 cm^{-1} appear, which could be associated with the metal−N stretch of the imido complex. At 2245 cm^{-1}, the C−N vibration of the coordinated acetonitrile is again observed. The results are also collected in Table 1.

A DFT frequency analysis of the model $[Mo(N)(NCCH_3)(diphos)_2]^+$ (**VI**) for the trans nitrilo−nitrido system predicts a frequency of 1088 cm^{-1} for the metal−N vibration. On the basis of a comparison with the other calculated frequencies, this would support our assignment of the shoulder at 1016 cm^{-1} to the metal−N stretch. The corresponding analysis for the imido system, **VI*H**$^+$, leads to frequencies of 913 cm^{-1} for the metal−N stretch and 3059 cm^{-1} for the N−H stretch. Thus the frequency of the metal−N vibration is, in this case, predicted too low compared to the experimental value.

DFT Geometry Optimizations. The optimized structure of the simplified model $[Mo(N)(N_3)(diphos)_2]$ (**I**) (diphos = $PH_2CH_2CH_2PH_2$) is shown in Figure 4. In this case, the azido ligand forms an almost linear unit together with the metal center and the trans nitrido ligand (∠Mo−N−N = 174.6°). This agrees with the crystal structure of the complex $[Mo(N)(N_3)(dppe)_2]$ determined by Dilworth et al.[24] Apart from minor discrepancies, the bond lengths resulting from the optimization also agree with the X-ray structural analysis.

(24) Dilworth, J. R.; Dahlstrom, P. L.; Hyde, J. R.; Zubieta, J. *Inorg. Chim Acta* **1983**, *71*, 21.

Table 3. Comparison of Important Internal Coordinates of Optimized Structures[a]

	I	I (^{3}E exc. st.)	I*H$^+$	III	III*H$^+$	VI	VI*H$^+$
N−H			1.021		1.024		1.024
Mo−N	1.711	1.792	1.763	1.701	1.742	1.690	1.729
Mo−α	2.295	2.403	2.059	2.781	2.570	2.629	2.353
α−*β*	1.230	1.233	1.233			1.174	1.174
β−*γ*	1.195	1.199	1.181			1.464	1.462
Ø **Mo−P**	2.560	2.56 (fixed)	2.590	2.551	2.573	2.572	2.593
H−N−Mo			179.7		179.9		179.6
N−Mo−α	179.6	173.8	179.8	179.9	179.9	178.8	179.7
Mo−α−*β*	174.6	127.1	179.1			178.1	179.8
α−*β*−*γ*	179.9	179.1	179.9			179.7	179.9
Ø **N−Mo−P**	96.0	96.0 (fixed)	94.5	99.3	98.8	94.2	95.8
Ø**ring P−Mo−P**	79.8	80.6	79.6	79.8	79.8	79.4	79.4
Ø**free P−Mo−P**	99.0	98.2	99.8	97.2	97.5	100.0	99.5

[a] α, *β*, and *γ* are the atoms of the trans ligand; the distances are given in Å and the angles in deg.

The metal−nitrido distance is calculated to be 1.711 Å, which is somewhat too short with respect to the experimentally determined value (1.79(2) Å). The metal−N(azido) distance, in turn, is calculated to be 2.295 Å, which is somewhat too long with respect to the observed value (2.20(2) Å).

In additon to the optimization of the singlet ground state, the triplet excited state ^{3}E of **I** was geometry optimized. As an unrestricted optimization was found to lead to dissociation of one phosphine ligand, the N−metal−P angles and the metal−P bond distances were fixed. This way, the triplet state, which results from a one-electron HOMO−LUMO excitation, could be optimized. The spin density in the triplet excited state was found to be 1.48 for the metal and 0.45 for the nitrido−N. The metal−N bond is elongated by 0.081 Å because of the population of the π^* orbital. Moreover, the slight bending of the azido ligand in the ground state is drastically enhanced. The metal−azide bond length increases from 2.295 to 2.403 Å, which corresponds to a weakening of this bond in the excited state.

A geometry optimization was also performed for the model of the imido complexes, $[Mo(NH)(N_3)(diphos)_2]^+$ (**I*H**$^+$). As evident from Figure 4, the azido−metal−N unit is almost linear ($\angle$Mo−N−N = 179.1°); moreover, the imido-hydrogen is bound in a linear fashion. The metal−N bond of 1.763 Å is only elongated by 0.05 Å, in comparison to the nitrido system, and the metal−azide distance is decreased by 0.236 Å to a length of 2.059 Å. The structural parameters agree well with the crystal structure of the imido complex [MoBr(NH)(dppe)$_2$]Br*MeOH obtained by Dilworth et al.[24] If a hydrogen bridge between the crystal solvent and a putative imido-hydrogen atom is assumed, a linear metal−N-H bond can be inferred from this structure as well. The linear arrangement of the imido-hydrogen is also supported by the crystal structures of alkylated complexes such as $[W(NCH_2CH_3)Cl(dppe)_2]PF_6$, which was crystallographically characterized by Seino et al.[25] In this case, the α-carbon atom is bound at a W−N−C angle of 172.80° to the metal center (i.e., again close to a linear fashion).

The optimized structures of the trans chloro complexes $[Mo(N)(Cl)(diphos)_2]$ (**III**) and $[Mo(NH)(Cl)(diphos)_2]^+$ (**III*H**$^+$) give comparable results. The metal−N distances are 1.701 and 1.742 Å, respectively, and hence, they are somewhat shorter than those in **I** and **I*H**$^+$. The metal center is markedly displaced from the phosphine plane, as can be inferred from the average nitride−metal−P angles (Table 3). The geometries of the models for the trans nitrile systems $[Mo(N)(NCCH_3)(diphos)_2]^+$ (**VI**) and $[Mo(NH)(NCCH_3)(diphos)_2]^{2+}$ (**VI*H**$^+$) can be inferred from Table 3 as well. In these cases, the metal−N bond is, with distances of 1.69 and 1.729 Å, respectively, markedly decreased. On the other hand, the distances from the metal center to the trans ligands (2.629 and 2.353 Å) are longer than in the analogous *trans*-azido systems.

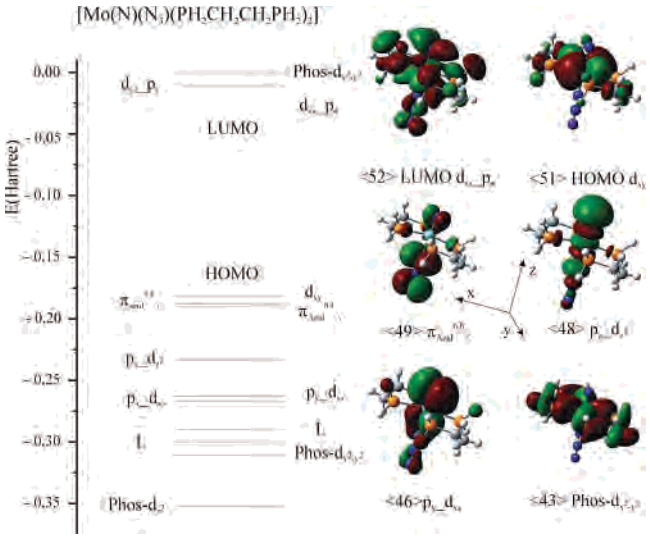

Figure 5. MO diagram of $[Mo(N)(N_3)(PH_2CH_2CH_2PH_2)_2]$ (**I**) with contour plots of some important orbitals.

MO Schemes. Figure 5 presents the MO scheme and some important orbitals of **I**; charge decompositions of important molecular orbitals are collected in Table S1 (Supporting Information). The HOMO of **I** corresponds to the metal−ligand nonbonding d_{xy} orbital. At lower energy, the degenerate π_{azide} orbitals in the *x* and *y* directions are located; they are nonbonding with respect to the metal. Then, the metal−ligand bonding MOs follow; they are involved in the metal−nitride triple bond. These comprise the σ-bonding orbital p_z–$d_{z^2} \equiv \sigma$ and the degenerate π-bonding orbitals p_x–$d_{xz} \equiv \pi_x$ and p_y–$d_{yz} \equiv \pi_y$. The corresponding metal−ligand

(25) Seino, H.; Tanabe, Y.; Ishii, Y.; Hidai, M. *Inorg. Chim. Acta* **1998**, *280*, 163.

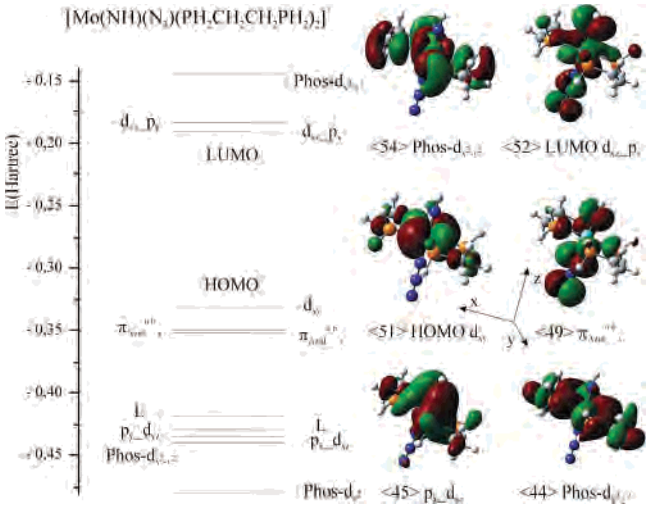

Figure 6. MO diagram of $[Mo(NH)(N_3)(PH_2CH_2CH_2PH_2)_2]^+$ (**I*H**$^+$) with contour plots of some important orbitals.

antibonding combinations $d_{xz}-p_x \equiv \pi_x^*$ and $d_{yz}-p_y \equiv \pi_y^*$ form the LUMO and the LUMO+1 of the complex. Evidently, the degeneracy of these orbitals is lifted through the presence of the bidentate equatorial phosphine ligands. NPA charge analysis reveals a molybdenum p contribution of 32% for the π_x^* orbital and one of 25% for the π_y^* orbital. The presence of d−p mixing accounts for the comparatively high intensity of the HOMO−LUMO transition (see below).

Figure 6 shows the MO scheme and the most important orbitals of the imido complex **I*H**$^+$. In analogy to the parent nitrido system **I**, the HOMO corresponds to the d_{xy} orbital; HOMO−1 and HOMO−2 correspond to the π_{azide} orbitals as discussed above. An important difference, compared to the nitrido complex, is observed for the metal−N σ-bonding orbital which shifts below the metal−ligand π-bonding orbitals π_x and π_y. Again the corresponding π-antibonding combinations, π_x^* and π_y^*, form the LUMO and the LUMO+1 of the complex. The charge decompositions indicate that these orbitals now only have 5 and 2% Mo p character (Table S2 in Supporting Information). Because of the protonation, the energy of these orbitals thus has decreased so much that the higher-lying Mo p orbitals are not admixed any more to a significant degree. Correspondingly, the intensity of the n → π^* transition in this case is comparable to that of an ordinary ligand-field band (see below).

Electronic Absorption and Emission Spectroscopy. In Figure 7, optical absorption spectra of $[Mo(N)(N_3)(depe)_2]$ (**5**) in thf solution are presented. The UV region exhibits two intense absorptions at 300 and 250 nm, and in the visible region, a weaker absorption band is found at 398 nm. The latter band is also present in the solid-state spectrum of compound **5** pressed between two sapphire plates (Figure S4, Supporting Information). When the sample is cooled from room temperature to 10 K, a vibrational structure appears on top of the 398 nm band. This is presented in Figure 8 along with a Gaussian fit of the band shape. The 398 nm band is assigned to the HOMO−LUMO transition which corresponds to the transfer of an electron from d_{xy} to $d_{xz}-p_x$

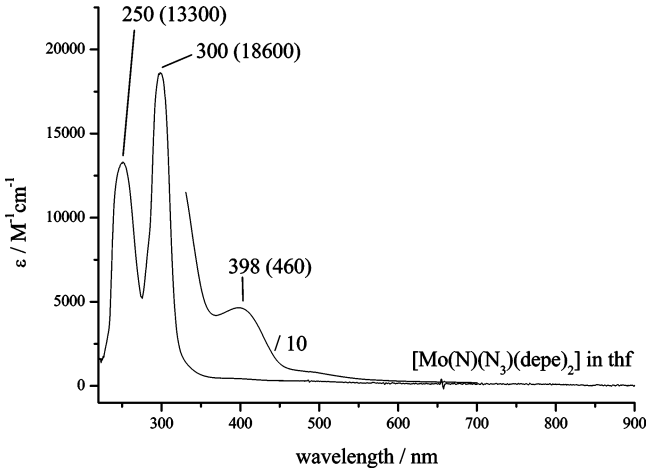

Figure 7. UV−vis spectra of $[Mo(N)(N_3)(depe)_2]$ (**5**) in thf.

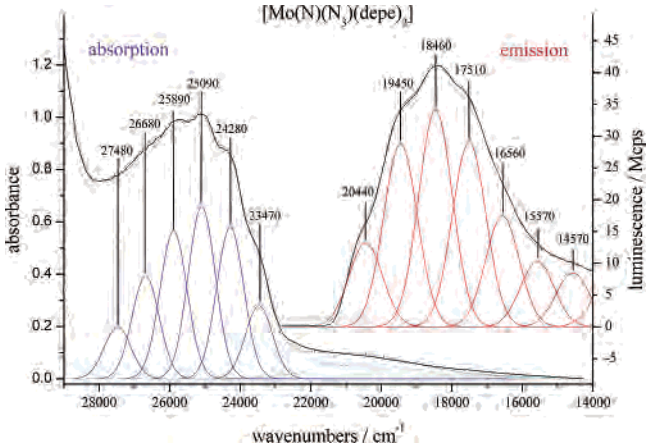

Figure 8. UV−Vis and luminescence spectra of $[Mo(N)(N_3)(depe)_2]$ (**5**) along with fit of the progression.

(π_x^*), the low-energy component of the $^1A_1 \rightarrow {}^1E$ transition. The TD-DFT calculation based on the simplified model $[Mo(N)(N_3)(diphos)_2]$ (**I**) calculates this singlet → singlet transition to be at 401 nm, in excellent agreement with the experimental observation. The transition from the d_{xy} orbital into the $d_{yz}-p_y$ (π_y^*) orbital (i.e., the higher-energy component of the $^1A_1 \rightarrow {}^1E$ transition) is calculated to be at 370 nm but with a much lower intensity (Table S3, Supporting Information) Another absorption band is found at 330 nm (Figure S4). This is assigned to a ligand field transition, either $d_{xy} \rightarrow d_{x^2-y^2}$ or $d_{xy} \rightarrow d_{z^2}$.[26] Alternatively, it could be assigned to the high-energy component of $^1A_1 \rightarrow {}^1E$. Nevertheless, its line width is much smaller than that of $d_{xy} \rightarrow d_{xz}-p_x$, and it does not exhibit a progression. At lower energy, an absorption band of much weaker intensity is observed and assigned to a spin-forbidden transition from the singlet ground state to the ^3E excited state.

Because the d_{xy} orbital is nonbonding and the d_{xz}/d_{yz} orbitals are antibonding with respect to the nitrido ligand, the singlet and triplet transitions have n → π^* character, and the metal−ligand bond length is increased in the excited states. This excited-state displacement in turn acts to excite the metal−N vibrations which appear as a progression in

(26) Bendix, J.; Bøgevig, A. *Inorg. Chem.* **1998**, *37*, 5992.

the singlet → singlet absorption band. The Gaussian fit of the line shape gives a spacing of 810 cm^{-1} which corresponds to the metal−N frequency in the excited state. The intensities of the individual transitions from the zero-point level of the ground state to the *n*th vibrational level of the excited state are determined by a Poisson distribution, as expressed by the equations

$$\frac{I_{0n}}{I_{0n-1}} = \frac{S}{n} \text{ and } \frac{I_{0n}}{I_{00}} = \frac{S_n}{n!} \quad (1)$$

S is the Huang−Rhys factor which gives the excited-state displacement, ΔQ, in terms of quanta of the corresponding vibration

$$Sh\nu = 1/2k'\Delta Q^2 \quad (2)$$

The Gaussian fit gives $S = 2.15$. Furthermore, by application of the excited-state frequency of 810 cm^{-1} in the normal coordinate analysis, an excited-state force constant, k', of 4.9 mdyn/Å is determined. Substitution of these values, in turn, into eq 2 gives an excited-state displacement, ΔQ, of 0.12 Å, which is in very good agreement with the theoretical prediction ($\Delta Q = 0.08$ Å, cf Table 3).

In addition to the absorption spectrum, Figure 8 also shows the emission spectrum of compound **5**. The luminescence is strongly temperature dependent, and at 11 K, it also shows a vibrational structure. The corresponding vibrational frequency is connected with the electronic ground state and is determined to be 980 cm^{-1}, in agreement with the results of the IR and Raman spectroscopy (vide supra). From the analysis of the intensity distribution of the luminescence with a Gaussian fit, a Huang−Rhys factor of 2.25 is derived. The corresponding horizontal displacement, ΔQ, is determined to 0.11 Å, in very good agreement with the value obtained from the absorption profile. Importantly, the $0 \leftrightarrow 0$ transitions of the absorption and emission spectrum of **5** do not coincide but exhibit an energy difference of 3030 cm^{-1}, indicating that the electronic states involved in absorption and luminescence are different. If the absorption band is assigned to the spin-allowed $d_{xy} \rightarrow d_{xz-}p_x$ singlet → singlet transition and the emission band to the spin-forbidden $d_{xz-}p_x \rightarrow d_{xy}$ triplet → singlet transition, the 3030 cm^{-1} energy difference corresponds to the energy gap between the (low-symmetry split) ^1E and the ^3E excited states.

The UV−vis absorption spectrum of the protonated complex $[Mo(NH)(N_3)(depe)_2]BPh_4$ (**5*HBPh$_4$**) is shown in Figure 9. Again, two high-energy bands can be identified (at 236 and 290 nm) which are shifted toward the UV region with respect to the parent complex **5**. In contrast, the low-energy n → π^* transition is shifted toward the IR region and now is found at 518 nm. This transition was calculated by TD-DFT applied to the **I*H**$^+$ model at 523 nm, again in excellent agreement with the experiment. As already mentioned, the intensity of this transition ($\epsilon = 145$ M^{-1} cm^{-1}) is typical for a ligand-field transition, whereas the intensity of the corresponding n → π^* transition in the parent compound ($\epsilon = 460$ M^{-1} cm^{-1}) is unusually high. We attribute this high intensity in the nitrido complex to extensive

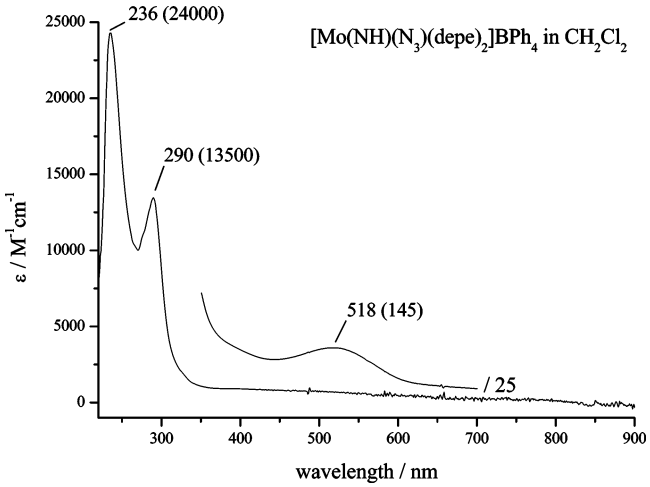

Figure 9. UV−vis spectra of $[Mo(NH)(N_3)(depe)_2]BPh_4$ (**5*HBPh$_4$**) in CH_2Cl_2.

d−p mixing which is markedly reduced in the corresponding imido system because of the increased effective nuclear charge on the metal (vide supra).

The absorption spectra of $[Mo(NH)(Cl)(dppe)_2]Cl$ (**3*HCl**) and $[W(NH)(Cl)(dppe)_2]Cl$ (**4*HCl**) have already been published by Henderson et al.[27] Here the n → π^* transitions were found at 525 and 488 nm, respectively. The TD-DFT calculation, based on model complex **III**, predicts an energy of 530 nm for this transition. Unfortunately, the n → π^* transition energy of the parent complex $[W(N)(Cl)(dppe)_2]$ (**4**) could not be exactly determined because of a new intense band which appears in complexes with aromatic phosphine ligands. We attribute this band to a transition from the metal to the phenyl phosphine group. In the corresponding alkyl phosphine complexes, this transition also exists but probably is at a much higher energy.[6,28] In the case of complex **4**, the metal−phosphine CT band appears at 360 nm. From the appearance of a weak shoulder, the much less intense n → π^* transition of **4** may be located around 400 nm, which would be in agreement with the TD-DFT calculation predicting a transition energy of 392 nm for this system.

Figure 10 presents the UV−vis absorption spectra of the nitrido nitrile compound $[Mo(N)(NCCH_3)(dppe)_2]BPh_4$ (**6**). The CT transition from the metal to the phosphine ligands is found at 330 nm. In comparison with complex **5**, which carries an anionic ligand trans to the nitrido group, the n → π^* transition is shifted to lower energy (450 nm). The TD-DFT calculation based on model complex **VI** predicts this transition at 437 nm, in good agreement with the experimental result. The measured energy shift of the HOMO−LUMO transition upon substitution of an anionic trans ligand by a neutral acetonitrile reflects two antagonistic effects: on one hand, the energy of the π^* orbitals is increased because of the strengthening of the metal−N bond, as can be inferred from the increase of the metal−N vibration frequency (vide

(27) (a) Henderson, R. A.; Davies, G.; Dilworth, J. R.; Thorneley, R. N. F. *J. Chem. Soc., Dalton Trans.* **1981**, 40. (b) Henderson, R. A. *J. Chem. Soc., Dalton Trans.* **1983**, 51.
(28) (a) George, T. A.; Busby, D. C.; Iske, S. D. A., Jr. *Inorg. Organomet. Photochem.* **1978**, 147. (b) Bossard, G. E.: Busby, D. C.; Chang, M.; George, T. A.; Iske, S. D. A., Jr. *J. Am. Chem. Soc.* **1980**, *102*, 1001.

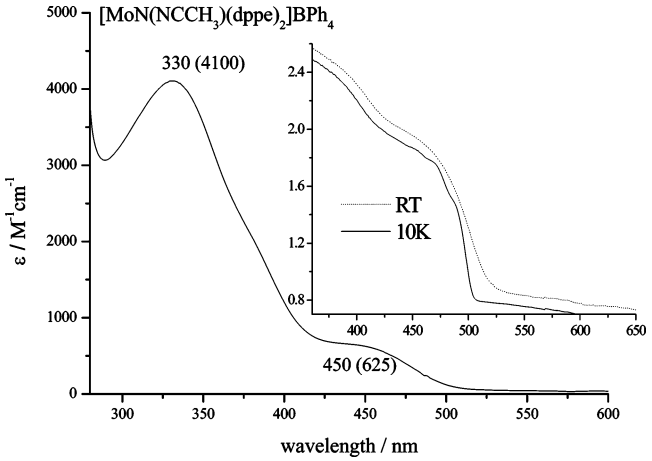

Figure 10. UV−vis spectrum of $[Mo(N)(NCCH_3)(dppe)_2]BPh_4$ (**6**) in CH_3CN. The inset shows the UV−vis spectrum of the pure compound pressed between sapphire plates.

Table 4. Calculated and Experimental $d_{xy} \rightarrow d_{xz-}p_x$ ($n \rightarrow \pi^*$) Transition Energies[a]

	I	I*H$^+$	III	III*H$^+$	VI	VI*H$^+$
TD-DFT	401	523	392	530	437	596
exptl	398 (depe)	518 (depe)	∼400 (dppe)	525[27] (dppe)	450 (dppe)	525 (dppe)

[a] All data given in nm.

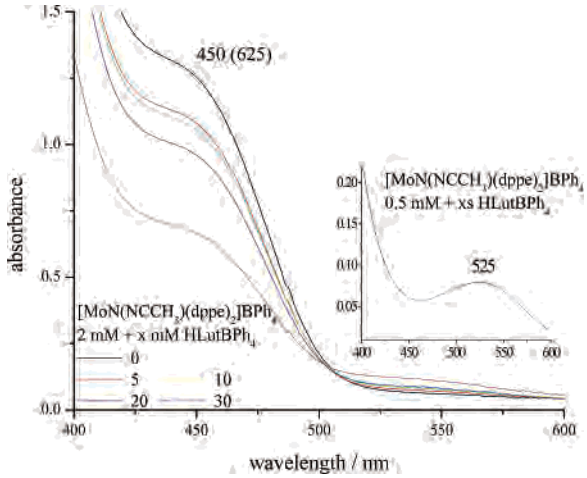

Figure 11. UV−vis spectrum of $[Mo(N)(NCCH_3)(dppe)_2]BPh_4$ (**6**) in CH_3CN after the addition of different amounts of $[HLutBPh_4]$. The inset shows the UV−vis spectrum of **6** with a great excess of acid.

supra). On the other hand, the energy of these orbitals is lowered because π donation of the trans ligand is eliminated. This effect obviously exceeds the first one in magnitude and leads to the observed red shift of the $n \rightarrow \pi^*$ transition. The inset of Figure 10 shows the solid-state spectrum of compound **6** recorded at 10 K. Again, a progression is visible, but this time spectral resolution is not good enough to allow further analysis. The results of the TD-DFT calculations and the experimental energies of the $n \rightarrow \pi^*$ transition are collected in Table 4.

Spectrometric Determination of pK_a. Figure 11 shows the absorption spectra of a 2 mM solution of **6** before and after the addition of different amounts of acid ($HLutBPh_4$). Evidently the signal at 450 nm decreases and the signal at 525 nm increases in intensity, reflecting the conversion of the nitrido to the imido complex. TD-DFT predicts the $n \rightarrow \pi^*$ transition in the imido nitrile model complex **VI*H**$^+$ at 597 nm, in fair agreement with the experimental result. The inset in Figure 11 shows the spectrum of a dilute solution of **6** in the presence of a large excess of acid. In this case an approximately complete conversion of **6** to its protonated counterpart, $[Mo(NH)(NCCH_3)(dppe)_2](BPh_4)_2$ (**6*HBPh**$_4$), is observed. In the intermediate range, the acid strength of the protonated complex **6*HBPh**$_4$ can be determined by the equation[29]

$$\Delta pK_a = pK_a(\mathbf{6*HBPh_4}) - pK_a(HLutBPh_4) = \log\left(\frac{[\mathbf{6*HBPh_4}][Lut]}{[HLutBPh_4][\mathbf{6}]}\right) \quad (3)$$

In acetonitrile, the pK_a of complex **6*HBPh**$_4$ differs from lutidinium by 1.7 units. On the basis of a pK_a of lutidinium of 6.7[29] in water, a pK_a value of 5 is derived for **6*HBPh**$_4$. This is much lower than that determined for imido complexes with anionic trans ligands.[27] For the complex $[Mo(NH)(F)(dppe)_2]BF_4$, for example, a pK_a value of 12.7 was determined. This result indicates that the basicity of the nitrido N drastically decreases upon exchange of an anionic to a neutral trans ligand. Correspondingly, the conversion of **6** to its protonated counterpart using the weak acid $HLutBPh_4$ is found to be incomplete in solutions containing a higher concentration of **6**. On the other hand, the reduction potential should increase upon substitution of the *trans*-halide by a *trans*-nitrile group (i.e., become less negative), as shown in the next section.

Table 5. Peak Potentials for the Reduction of Nitrido and Imido Complexes with Anionic and Neutral trans Ligands

	E_p^{red} (V vs Fc^+/Fc)
$[Mo(N)(NCCH_3)(dppe)_2]^+$	−1.53
$[Mo(N)(Cl)(dppe)_2]$	<−2.4
$[Mo(NH)(Cl)(dppe)_2]^+$	−2.09[11]
$[Mo(NEt)(Cl)(dppe)_2]^+$	−2.21[11]
$[Mo(NEt)(NCCH_3)(depe)_2]^{2+}$	−1.5[30]

Electrochemical Investigation of 6. For Mo/W nitrido systems with anionic trans ligands no reduction potential could be determined within the stability range of ordinary solvents and electrolytes, respectively. In contrast, electrochemical data for protonated and alkylated systems have been obtained (cf., Table 5).[11] Figure 12 shows a cyclovoltammogram of the trans nitrido nitrile complex **6**, indicating an irreversible reduction at −1.53 V vs ferrocenium/ferrocene. Furthermore, two irreversible oxidations are observed at 65 and 540 mV. An inspection of Table 5 shows that the replacement of a trans halide by acetonitrile shifts the reduction potential by ∼1 V toward more positive values. In fact, the reduction potential of *nitrido* complex **6** is comparable to that of the *trans*-alkyl*imido* acetonitrile complex $[Mo(NEt)(NCCH_3)(depe)_2](OTf)_2$, which has depe instead of dppe coligands.[30] It thus can be concluded that

(29) Kaljurand, I.; Kütt, A.; Sooväli, L.; Rodima, T.; Mäemets, V.; Leito, I.; Koppel, I. A. *J. Org. Chem.* **2005**, *70*, 1019.
(30) Sivasankar, C.; Böres, N.; Peters, G.; Habeck, C. M.; Studt, F.; Tuczek, F. *Organometallics* **2005**, *24*, 5393.

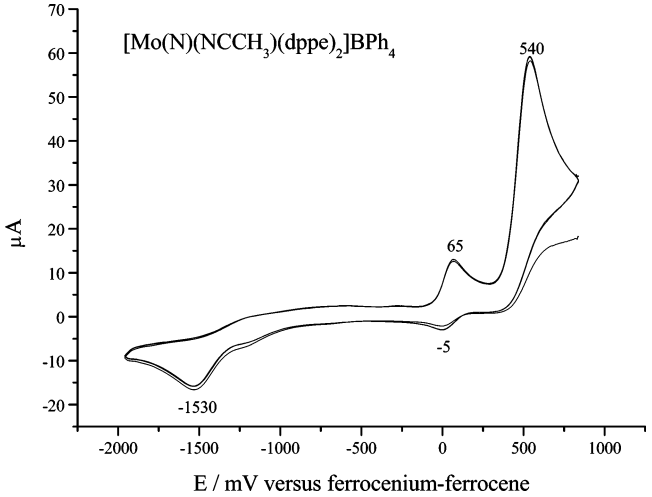

Figure 12. Cyclic voltammogram of $[Mo(N)(NCCH_3)(dppe)_2]BPh_4$ (**6**) (0.5 mM) in CH_3CN, 0.1 M $(NBu_4)PF_6$ at 25 °C and a scan rate of 100 mV s^{-1}.

molybdenum trans imido− or alkylimido−acetonitrile complexes with *dppe* coligands should even be reducible at potentials above −1.5 V vs Fc^+/Fc.

4. Discussion

The preceding sections continue our line of theoretical and spectroscopic studies on the intermediates of the Chatt cycle. Previous publications have dealt with the protonation of the coordinated N_2 ligand in Mo(0) and W(0) diphosphine complexes and the subsequent N−N splitting process.[6,7,10] Heterolytic cleavage of the N−N bond in Mo(II) and W(II) systems generates the corresponding Mo(IV) and W(IV) nitrido and imido systems which have to be protonated and reduced to the zero-valent state to produce NH_3 and rebind N_2. A problem of the Chatt cycle are the strongly negative potentials (down to −2.3 V vs Fc^+/Fc)[11] involved in these processes. It is therefore of considerable interest to investigate in more detail the electronic structures of these systems and to explore possibilities to shift these potentials to less negative values.

In the nitrido complexes with *trans*-azido and -chloro coligands, the metal−N stretch is observed at about 980 cm^{-1}, relatively independent of the nature of the trans ligand and the equatorial phosphine ligation. ^{15}N substitution in compound **4** causes an isotopic shift of this vibration to ∼950 cm^{-1}. A metal−N force constant of 7.065 mdyn/Å is determined using the QCB-NCA procedure. When the corresponding imido systems are generated by protonation, the metal−N stretching frequency is lowered to about 950−920 cm^{-1}. In this case, a relatively strong dependence on the nature of the counterion is observed. As evident from a highly complex vibrational structure in the N−H stretching frequency region, extensive hydrogen bonding occurs in imido complexes with chloro counterions. In this case, the metal−N stretching frequency is observed at ∼950 cm^{-1}. In the absence of hydrogen bonding (i.e., in the compounds with tetraphenylborate counterions), the metal−N(imido) stretch is observed at 925−920 cm^{-1}. On the basis of the latter value, a force constant of 6.7 mdyn/Å is derived. This indicates that protonation only causes a minor decrease (0.3 mdyn/Å) of the metal−N force constant. For both systems with chloride and BPh_4 counterions, deuteration causes a further decrease of the metal−N stretching vibration frequency by 30−40 cm^{-1}, reflecting the increased mass of the N−H moiety.

The vibrational-spectroscopic investigations of the nitrido and imido complexes are complemented by measurements of their electronic absorption and emission spectra. For this purpose, Mo and W complexes with depe ligands are better suited than corresponding dppe complexes as the latter exhibit low-energy metal → phosphine CT transitions which tend to obscure ligand-field (LF) transitions. Correspondingly, the molybdenum azido−nitrido complex $[Mo(N)(N_3)(depe)_2]$ (**5**) was found to give a clean LF spectrum which, in particular, exhibited the $d_{xy}(nb) \rightarrow d_{xz-}p_x(\pi_x^*)$ transition at 398 nm. The relatively high intensity of this spin-allowed n → π^* transition ($\epsilon = 460$ M^{-1} cm^{-1}) is ascribed to extensive d−p mixing. At lower energy, an absorption band of much weaker intensity is observed, which is assigned to the corresponding spin-forbidden transition from the singlet ground state to the lower-energy component of the ^3E (n → π^*) excited state. When the sample had cooled, a vibrational progression appears on top of the singlet → singlet absorption band. Its spacing, 810 cm^{-1}, corresponds to the metal−N stretching frequency in the ^1E (n → π^*) excited state. An excited-state force constant of 4.9 mdyn/Å is derived by inserting this frequency into the ground-state normal coordinate analysis. Moreover, a Franck−Condon analysis of this absorption feature gives a Huang−Rhys factor of 2.15 and an excited-state displacement of 0.12 Å.

Remarkably, a vibrational progression is found in the emission spectrum of compound **5** at low temperatures as well. To the best of our knowledge, this is the first luminescence spectrum of such a molybdenum−nitrido system.[31] In this case, a spacing of 980 cm^{-1} is observed which corresponds to the metal−N stretching vibration in the electronic ground state. Franck−Condon analysis of the emission line shape gives a Huang−Rhys factor of 2.25 and a displacement, ΔQ, of 0.11 Å, in good agreement with the absorption data. As the emission band is at comparable energy to the low-intensity spin-forbidden transition in the absorption spectrum, it is assigned to the phosphorescence from the lower-energy component of the $^3E(n \rightarrow \pi^*)$ excited state to the $^1A_1$ ground state. On the basis of the energy difference between the 0 ↔ 0 transitions in absorption and emission, the splitting between the ^1E and $^3E(n \rightarrow \pi^*)$ excited states is 3030 cm^{-1}. When the fact that this splitting corresponds to $6B + 2C$[32] is considered, it becomes clear that this system is highly covalent.[33,34] Upon protonation of

(31) Different combinations of research topics such as molybdenum/tungsten, nitrido, and luminescence/phosphorescence with SciFinder resulted in no relevant hits.
(32) Da Re, R. E.; Hopkins, M. D. *Inorg. Chem.* **2002**, *41*, 6973.
(33) With a literature value of $B = 682$ cm^{-1} for a Mo^{4+} ion and $C = 4B$, a splitting of 9548 cm^{-1} is evaluated.

the nitrido complexes the (n → π*) transition shifts to lower energy (518 nm); moreover, its intensity decreases considerably. The low-energy shift can be explained by a weaker π-antibonding interaction between the metal d_{xz}/d_{yz} orbitals and the p orbitals of the imido ligand, as compared to the nitrido system. The intensity decrease is attributed to a decrease in d−p mixing as a consequence of the increase in the effective nuclear charge of the M(IV) system.

Further insight into the electronic structure and spectroscopic properties of the nitrido and imido systems investigated in this study has been obtained by DFT calculations performed on the model systems $[Mo(N)(N_3)(diphos)_2]$ (**I**), $[Mo(N)(Cl)(diphos)_2]$ (**III**), $[Mo(N)(NCCH_3)(diphos)_2]$ (**VI**), $[Mo(NH)(N_3)(diphos)_2]^+$ (**I*H**$^+$), $[Mo(NH)(Cl)(diphos)_2]^+$ (**III*H**$^+$), and $[Mo(NH)(NCCH_3)(diphos)_2]^{2+}$ (**VI*H**$^+$). In the corresponding geometry-optimized structures, the metal−N distances are generally found somewhat too short. This is also reflected by the fact that the metal−N frequencies are calculated somewhat too high in energy. TD-DFT-calculations give n → π* transition energies which are in very good agreement with the experimental data. For the n → π* excited state of $[Mo(N)(N_3)(diphos)_2]$ (**I**), a partial geometry optimization has been performed. In good agreement with the experimental value, an elongation of the metal−N(nitrido) distance by 0.08 Å has been found. However, the metal−N(azido) distance increases as well (by 0.11 Å), and the bending of the azido ligand increases.

It is instructive to compare the properties of the Mo and W nitrido and imido systems to those of the corresponding oxo compounds which have been studied in detail by several groups.[26,32,35] Da Re and Hopkins have investigated a series of molybdenum oxo complexes of the type $[MoOL_4Cl]^+$ (L = $CNBu^t$, PMe_3, and 1/2dmpe).[32] The Mo−O stretching frequency of these ions (948−959 cm^{-1}) was essentially found to be insensitive to the nature and geometry of the equatorial ligands. However, the electronic absorption bands resulting from the $d_{xy} \rightarrow d_{xz}/d_{yz}$ n → π*(Mo−O) LF transition show a large dependence on the geometry of the equatorial ligation. Specifically, the $[MoO(CNBut)_4Cl]$ complex exhibits a single $^1[n \rightarrow \pi^*_{x,y}]$ band, whereas the spectra of both $[MoO(dmpe)_2Cl]^+$ and $[MoO(PMe_3)_4Cl]^+$ reveal separate $^1[n \rightarrow \pi^*_x]$ and $^1[n \rightarrow \pi^*_y]$ bands. Nitrido complex **5** is chemically related to these systems and therefore should have split singlet and triplet n → π* excited states; however, the magnitude of this splitting cannot be inferred from the spectroscopic data. It is clear that luminescence occurs from the lower-energy component of the ^{3}E excited state. From the almost identical line shapes in the absorption and emission spectra, we conclude that the absorption band corresponds to the electronic transition from $^1A_1$ to the lower-energy component of ^{1}E, in agreement with the prediction from TD-DFT. The higher-energy component of ^{1}E is not visible in the absorption spectrum. A possible explanation is the much lower intensity predicted for this transition by TD-DFT. Otherwise the absorption bands of the Mo−O systems have properties which are very similar to those of Mo−nitrido complex **5** (i.e., they show a vibronic spacing of ∼800 cm^{-1}, which is considerably lower than the ground-state Mo−O stretching frequency of ∼960 cm^{-1}), and Franck−Condon analysis gives an excited-state displacement, ΔQ, of ∼0.1 Å.

A major change in the spectroscopic properties and the reactivity of the nitrido complexes is observed upon exchange of the anionic trans ligands by acetonitrile. Most conspicuously, the metal−N(nitride) stretching frequency increases to 1016 cm^{-1}, reflecting a strengthening of the metal−nitrido bond. The n → π* transition now is found at 450 nm, shifting to 525 nm upon protonation. Furthermore, the reduction potential is shifted from more negative values to −1.53 V vs Fc^+/Fc which is close to the $E°$ value of decamethylchromocene used as a reductant in the Schrock cycle.[2] This drastically facilitates the reduction of the nitrido−nitrile system compared to its counterparts with anionic trans ligands which cannot be reduced at experimentally accessible potentials. Even less negative reduction potentials are expected for the corresponding imido systems $[Mo(NH)(NCCH_3)(dppe)]^{2+}$ and $[Mo(NR)(NCCH_3)(dppe)]^{2+}$ (for $[Mo(NEt)(CH_3CN)(depe)]^{2+}$ a reduction potential of −1.5 V has been determined,[30] but the corresponding dppe analogues should be reducible at less negative potentials).

Exchange of the anionic trans ligands by nitrile, on the other hand, also leads to a considerable decrease in basicity of the nitrido group. By titration experiments with $HLutBPh_4$, a pK_a value of 5.0 was determined for complex **6*HBPh$_4$**, which is much lower than that observed for corresponding systems with trans halide ligands (p$K_a \approx 10$).[27] Importantly, however, the nitrido group is still *basic enough* because protonation of **6,** even with the weak acid $HLutBPh_4$, proceeds with an equilibrium constant K_a of 1/50. Conversion to a free reaction enthalpy gives a corresponding $\Delta G°$ value of +10 kJ/mol which does not represent an appreciable barrier in the transformation of coordinated nitride to ammonia.

In summary, the electronic structures of a series of Mo and W nitrido and imido complexes have been determined and their spectroscopic properties have been investigated in detail. The experimental and theoretical results have been correlated to the observed reactivities, in particular reduction potentials and Brønsted basicities. In this way, it has been found that the replacement of anionic trans ligands by acetonitrile causes a pronounced shift in the reduction potentials toward less negative values, thus rendering these systems promising intermediates for a catalytic realization of the Chatt cycle. In this respect, it is advantageous that the activation of N_2 in complexes with *trans*-nitrile ligands is higher than in corresponding *trans*-bis(dinitrogen) complexes.[36] The trade-off for the easier reducibility is a considerable decrease of the basicity of the nitrido group which,

(34) Griffith, J. S. *The Theory of Transition-Metal-Ions*; Cambridge University Press: Cambridge, U.K., 1971.
(35) Isovitsch, R. A.; Beadle, A. S.; Fronczek, F. R.; Maverick, A. W. *Inorg. Chem.* **1998**, *37*, 4258.
(36) Habeck, C. M.; Lehnert, N.; Näther, C.; Tuczek, F. *Inorg. Chim. Acta* **2002**, *737C*, 11.

however, should not present a serious obstacle to further conversion of the nitrido complex along the Chatt cycle.

Acknowledgment. Dedicated to Prof. Dr. Hansgeorg Schnöckel on the occasion of his 65th anniversary. F.T. thanks DFT Tu58/12-1 and FCI for financial support. K.M. thanks U. Cornelissen for help with the spectroscopic measurements.

Supporting Information Available: Tables of charge contributions, n $\rightarrow \pi^*$ transitions, and NPA charges, a description of the charge analysis, and figures showing Raman, IR, and UV−vis spectra. This material is available free of charge via the Internet at http://pubs.acs.org.

IC060141N